COOPERATION

Grant Agreement No. 611373

CADDY

Cognitive Autonomous Diving Buddy

FP7-ICT-2013-10

D4.3. Implementation of cooperative navigation algorithms

Due date of deliverable: 05/2016

Actual submission date: 05/2016

Start date of project: 01 January 2014 Duration: 36 months

Organization name of lead contractor for this deliverable: IST

Revision: version 1

Dissemination level		
PU	Public	x
PP	Restricted to other programme participants (including the Commission Services)	
RE	Restricted to a group specified by the consortium (including the Commission Services)	
CO	Confidential, only for members of the consortium (including the Commission Services)	

Contents

1 Outline of the deliverable

This deliverable describes the navigation algorithms designed and implemented in the scope of the CADDY project. Two categories of filters were studied, on one hand resorting only to AHRS, range measurements and exchanged data, on the other hand taking advantage of all the common expensive sensors as USBL and DVL.

2 Navigation filter using USBL and DVL measurements (IST)

The system architecture for both surface and underwater vehicle can be seen in the diagram of Figure 2.1.

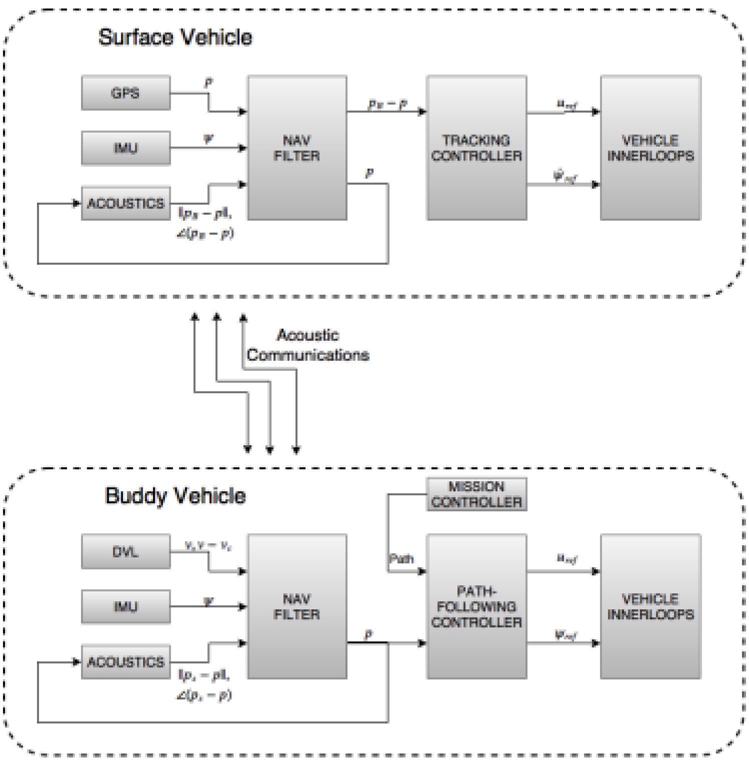

Figure 2.1 - System architecture diagram

Both the leader and the follower vehicles ran an Extended Kalman Filter (EKF) to independently estimate the positions and velocities of both vehicles in the experiment. The surface vehicle must estimate the position of the underwater one in order to track it; the underwater vehicle needs to estimate the position of the surface one in order to use the USBL measurements (range and bearing between vehicles) to infer its own position. Note that bearing and range measurements are used by the filter as separate measurements, so that the variance of the bearing measurement noise can be assumed much bigger than that of the range. Indeed, the filter was set to be only slightly affected by bearing measurements, reducing the effect of big deviations.

The state of the filter was defined as $x = [p, v, v_c, p_1, v_1]^T$, each of these entries is a 2D vector where p is the estimated global position (x, y), v the inertial velocity, v_c the velocity of the current, and the number indices refer to other agents estimates.

The state transition model is shown in Figure 2.2 and a list of the updates appears in Figure 2.3.

$$\begin{bmatrix} \dot{\boldsymbol{p}} \\ \dot{\boldsymbol{v}} \\ \dot{\boldsymbol{v}}_c \\ \dot{\boldsymbol{p}}_1 \\ \dot{\boldsymbol{v}}_1 \\ \vdots \\ \dot{\boldsymbol{p}}_n \\ \dot{\boldsymbol{v}}_n \end{bmatrix} = \begin{bmatrix} \boldsymbol{v} \\ \boldsymbol{0} \\ \boldsymbol{0} \\ \boldsymbol{v}_1 \\ \boldsymbol{0} \\ \vdots \\ \boldsymbol{v}_n \\ \boldsymbol{0} \end{bmatrix}$$

Figure 2.2 - State transition model

$$\begin{aligned} y_{\text{DVL bottom track}} &= \boldsymbol{v} \\ y_{\text{DVL water track}} &= \boldsymbol{v} - \boldsymbol{v}_c \\ y_{\text{GPS}} &= \boldsymbol{p} \\ y_{\text{water velocity from thrusters}} &= \boldsymbol{v} - \boldsymbol{v}_c \\ y_{\text{received position of vehicle i}} &= \boldsymbol{p}_i \\ y_{\text{received velocity of vehicle i}} &= \boldsymbol{v}_i \\ y_{\text{range to vehicle i}} &= \|\boldsymbol{p}_i - \boldsymbol{p}\| \\ y_{\text{bearing to vehicle i}} &= \angle(\boldsymbol{p}_i - \boldsymbol{p}) \end{aligned}$$

Figure 2.3 - Updates for the filter

Note that despite the fact that the filter can be used for n agents, it was only used for 2 vehicles. Delays were taken into account by keeping a buffer of previous measurements with their correspondent state and covariance. Moreover, outliers are rejected using a normalized residual validation gate which is then displayed real-time on the console, if a Wi-Fi link to the vehicle is available.

The underwater vehicle relies mainly on DVL measurements for short-term navigation, so its estimate of the surface vehicle position is not so critical. However, the estimate of the underwater vehicle computed at the surface one is important, since the tracking is based only on this estimate. We focus here on illustrating this.

Figure 2.4 shows the residual of range measurements, i.e. the difference between each range measurement and the expected range value from the EKF state. Note that the performance is reasonable since these measurements are obtained only approximately once every 6 seconds and the surface vehicle has no extra information regarding the motion of the underwater one. In particular, the velocity of the underwater vehicle is very hard to estimate with such scarse data. In the future, the underwater vehicle will broadcast its velocity and we expect the performance of this filter to improve.

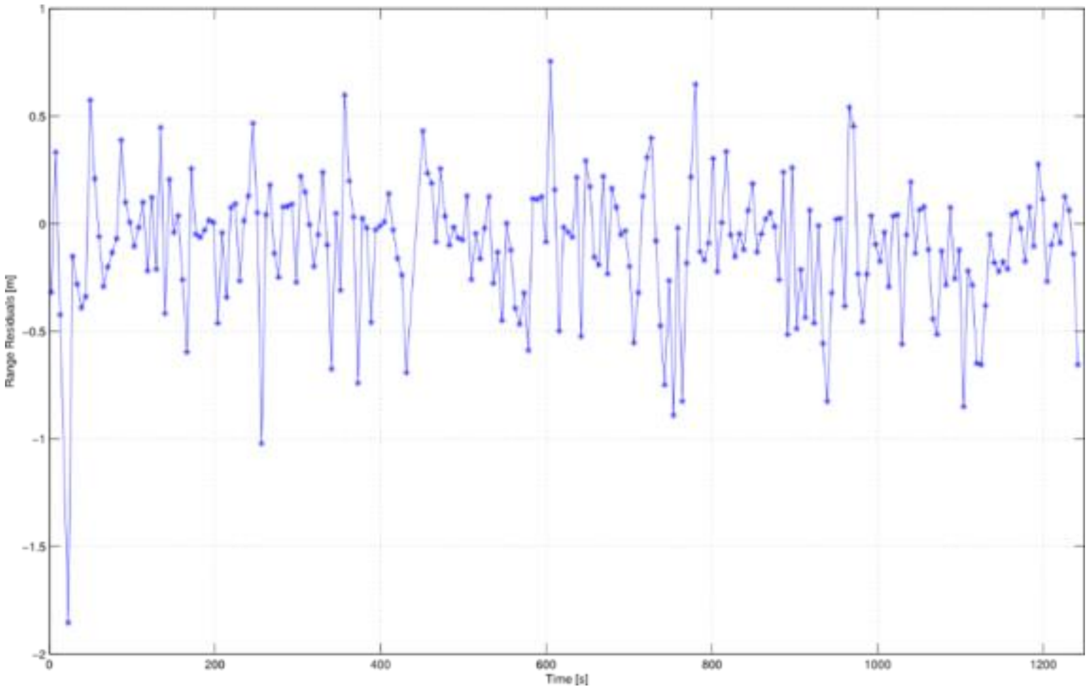

Figure 2.4 - Range residuals on a filter update

3 Single Beacon Navigation (IST)

Autonomous underwater vehicles (AUVs) have supplanted the conventional methods for the ocean exploration to carry out a wide range of scientific and commercial missions. For the successful execution of these missions, position estimation of vehicles is a critical component. Vehicle positioning and underwater target localization systems pose a greater challenge in marine robotics due to absence of GPS. As an alternative, acoustic based methods such as LBL (Long Baseline), SBL (Short Baseline), and USBL (Ultra Short Baseline). With the increasing level of autonomy, there was a need for the development of reliable and cost effective underwater navigation systems and, recently, there has been a growing interest aimed at the implementation of integrated motion planning algorithms that can adapt to the circumstances as the mission unfolds. In particular, while a fleet of AUVs operating autonomously, the position estimate based on the noisy measurements of the less accurate sensors significantly depends on the type of the motion imparted of the AUVs. Thus, due to the limited resources of AUVs, the accuracy of the localization can be improved by imposing proper motion on the individual AUVs.

In this context, we address the problems of range-based marine vehicle positioning and target localization with or without ocean currents. *Vehicle positioning* aims to estimate the positions of one or more vehicles from a sequence of range measurements to fixed or moving acoustic beacons, the positions of which are known functions of time. In this context, the vehicles must execute sufficiently exciting maneuvers while avoiding inter-vehicle collisions, so as to maximize the range-based information available for multiple vehicle positioning. In an estimation theory setting, the paper proposes a method to compute multiple vehicle trajectories so as to maximize the determinant of an appropriately defined Fisher Information matrix, subject to collision avoidance constraints. A numerical solution is proposed for the general case. Analytical solutions are obtained in the case of one vehicle and one beacon, when the latter undergoes trajectories that are straight lines, pieces of arcs, or a combination thereof. The theoretical analysis is complemented with practical experiments that focus on the dual problem of underwater target localization. The objective is to estimate the position of a moving underwater target by using range measurements between the target and a vehicle, called a *tracker*, undergoing a trajectory that can be measured on-line. The experimental set-up includes a surface and an autonomous underwater vehicle of the Medusa-class playing the roles of tracker and target, respectively. In the methodology adopted for system implementation the tracker runs three key algorithms simultaneously, over a sliding time window:

i) Tracker motion planning,
ii) Tracker motion control, and
iii) Target motion estimation based on range data acquired on-line.

The experimental results show that the strategies adopted for vehicle positioning and target localization hold considerable promise for practical system implementation.

Model

We consider a general scenario of p vehicles and q beacons scenario and model the each of the vehicle by the simple kinematics given by

$$\Sigma_{\mathrm{NC}}^{i}: \begin{aligned} \dot{\mathbf{p}}^{[i]} &= \begin{bmatrix} \cos(\chi^{[i]}) & -\sin(\chi^{[i]}) \\ \sin(\chi^{[i]}) & \cos(\chi^{[i]}) \end{bmatrix} \begin{bmatrix} v_1^{[i]} \\ 0 \end{bmatrix} \\ \dot{\chi}^{[i]} &= r^{[i]} \end{aligned}$$

where $\mathbf{p}^{[i]} \in \mathbb{R}^2$ is the inertial position of the i^{th} vehicle, $v^{[i]}$ is the linear body-speed of the i^{th} vehicle, $\chi^{[i]}$is the course angle of the i^{th} vehicle, and $r^{[i]}$ is the course-rate the i^{th} vehicle. The vehicle is equipped with acoustic sensors that measure distances to beacons whose position as a function of time is known in inertial frame. We are interested in estimating the initial position of each of the vehicles $\mathbf{p}_0^{[i]} \in \mathbb{R}^2$ using the ranges to the beacons that are corrupted by white Gaussian additive noise.

In the presence of constant, unknown ocean currents $\mathbf{v}_{\mathrm{c}} \in \mathbb{R}^2$ the equations are given by

$$\Sigma_{\mathrm{C}}^{i}: \begin{aligned} \dot{\mathbf{p}}^{[i]} &= \begin{bmatrix} \cos(\chi^{[i]}) & -\sin(\chi^{[i]}) \\ \sin(\chi^{[i]}) & \cos(\chi^{[i]}) \end{bmatrix} \begin{bmatrix} v_1^{[i]} \\ 0 \end{bmatrix} + \mathbf{v}_{\mathrm{c}} \\ \dot{\mathbf{v}}_{\mathrm{c}} &= \mathbf{0} \\ \dot{\chi}^{[i]} &= r^{[i]}. \end{aligned}$$

In this particular scenario, we are interested in estimating the initial position of each of the vehicles $\mathbf{p}_0^{[i]} \in \mathbb{R}^2$ and constant, unknown ocean currents $\mathbf{v}_\mathrm{c} \in \mathbb{R}^2$ the using the ranges to the beacons that are corrupted by white Gaussian additive noise.

Cost Function

The choice of cost functional is the Fisher information matrix (FIM), which is related to the lower bound achieved by an unbiased estimator. So, the aim is to maximize the Fisher information. To facilitate the derivation of the FIM we assume that inputs to vehicles are piecewise constant functions, that is, the surge speed and course rates are piecewise constant function.

First we assume that there is no ocean current. To this end, for each vehicle, we let $FIM_{\mathrm{NC}}^{[i]}\left(\mathbf{p}_0^{[i]}\right) \in \mathbb{R}^{2\times 2}$ denote the FIM. It can be shown that the overall FIM with m vehicles, i.e., $FIM_{\mathrm{NC}}\left(\mathbf{p}_0^{[1]},\cdots,\mathbf{p}_0^{[p]}\right) \in \mathbb{R}^{2p\times 2p}$, is nothing but the direct sum of the FIM of the each vehicles. With this, we define our cost function as

$$J_{\mathrm{NC}}(\mathbf{u}) \coloneqq \ln\left(\det\left(FIM_{\mathrm{NC}}\left(\mathbf{p}_0^{[1]},\cdots,\mathbf{p}_0^{[p]}\right)\right)\right).$$

Next, we assume that there are ocean currents. For each vehicle, we let $FIM_{\mathrm{C}}^{[i]}\left(\mathbf{p}_0^{[i]},\mathbf{v}_\mathrm{c}\right) \in \mathbb{R}^{4\times 4}$ denote the corresponding FIM and the overall FIM with m vehicles, i.e., $FIM_{\mathrm{C}}\left(\mathbf{p}_0^{[1]},\cdots,\mathbf{p}_0^{[p]},\mathbf{v}_\mathrm{c}\right) \in \mathbb{R}^{4p\times 4p}$, is the direct sum of the FIM of the each vehicles. Now our cost function becomes

$$J_{\mathrm{C}}(\mathbf{u}) \coloneqq \ln\left(\det\left(FIM_{\mathrm{C}}\left(\mathbf{p}_0^{[1]},\cdots,\mathbf{p}_0^{[p]},\mathbf{v}_\mathrm{c}\right)\right)\right).$$

In the above we have defined our cost function. Our aim now is to find the control input $\mathbf{u}$ that maximizes the cost function $J_{\mathrm{NC}}(\mathbf{u})$ in the absence of currents and $J_{\mathrm{C}}(\mathbf{u})$ in the presence of ocean currents. Mathematically,

$$\mathbf{u}_{\mathrm{NC}}^{*} = \max_{\mathbf{u}\in\mathcal{U}} J_{\mathrm{NC}}(\mathbf{u}) \quad \text{(Without currents)}$$

$$\mathbf{u}_{\mathrm{C}}^{*} = \max_{\mathbf{u}\in\mathcal{U}} J_{\mathrm{C}}(\mathbf{u}) \quad \text{(With currents).}$$

Solving the above optimal control problem is not easy. The derivation of FIM for the both of the set-ups are given in (Moreno-Salinas, et al. 2016)**Error! Reference source not found.** and (Crasta, et al. 2016). The reference (Moreno-Salinas, et al. 2016) provides a detailed construction of an analytical solution to the first optimal control problem (without currents) and it is implemented in real-time as explained in the later section.

In the sequel we focus on the case where there is no current. Borrowing results from matrix theory, it can be shown that the optimal value of the FIM for a single vehicle in the absence of currents is given by

$$FIM_{\mathrm{NC}}^{[i]}\left(\mathbf{p}_0^{[i]}\right) = \left(\frac{mq}{2\sigma^2}\right)\begin{bmatrix}1 & 0\\ 0 & 1\end{bmatrix}$$

where m and σ are the number of samples and the noise covariance, respectively (Here we assumed that all the sensors have the same covariance). Consequently, the overall optimal of the cost function is given by

$$\det\left(FIM_{\mathrm{NC}}\left(\mathbf{p}_0^{[1]},\cdots\cdot,\mathbf{p}_0^{[p]}\right)\right)=\left(\frac{mq}{2\sigma^2}\right)^p.$$

Now that we know the optimal value of the cost, our task is to find a trajectory, or equivalently, an input that achieve the optimal value of the cost. We have actually constructed an analytical solution that achieves the optimal control objective.

Algorithm

Figure shows the overall architecture of the algorithm. It has three components

i) Planner,
ii) Controller,
iii) Estimator.

Planner optimizes the cost functional (log of the determinant of the FIM) over a pre-fixed time horizon or number of samples and generates optimal positions. The planner uses the nominal speed for generating the optimal positions.

Controller executes the corresponding inputs, that is, body-speed and course-rate, to drive the vehicle to the next optimal position to acquire the range measurement. From the optimal position generated from the planner, controller finds the inputs that are compatible with the adopted model.

Finally, the *Estimator* estimates the position using the new range measurement. At the new optimal position the procedure is repeated. All these computations are implemented on the vehicle.

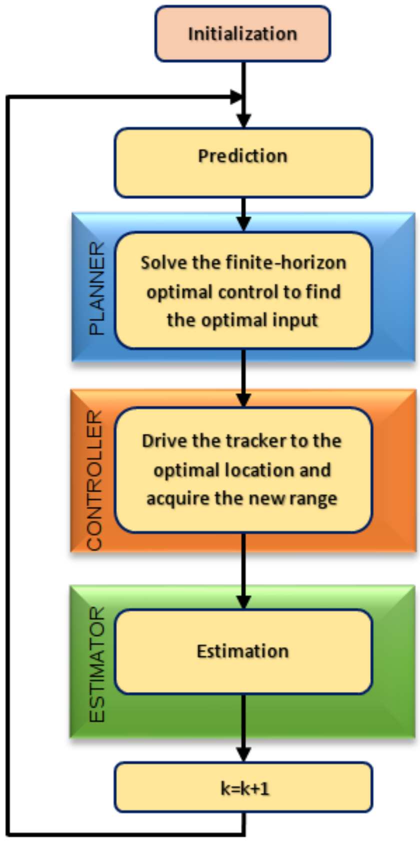

Figure 3.1 - Flow chart of the algorithm

4 Maximizing observability by using extremum seeking (UNIZG-FER)

Good underwater localization is of utmost importance for successful execution of all CADDY scenarios and therefore USBL systems are used to achieve that. Cheaper alternative is to use range only measurements. In such case unmanned surface vehicle (USV) is trying to execute trajectories informative enough in order to enhance observability of an underwater object, e.g. AUV or diver, which navigates itself by using only range measurements acquired by acoustic modems. We investigate the possibility of using extremum seeking (ES) scheme for online determining of informative enough beacon trajectories with lower computational effort. ES scheme is usually deployed when system model is not known very well or even completely unknown and its use for navigating autonomous vehicles towards an unknown source using measurements that indicate field intensity in certain point in environments without GPS signal is a common research.

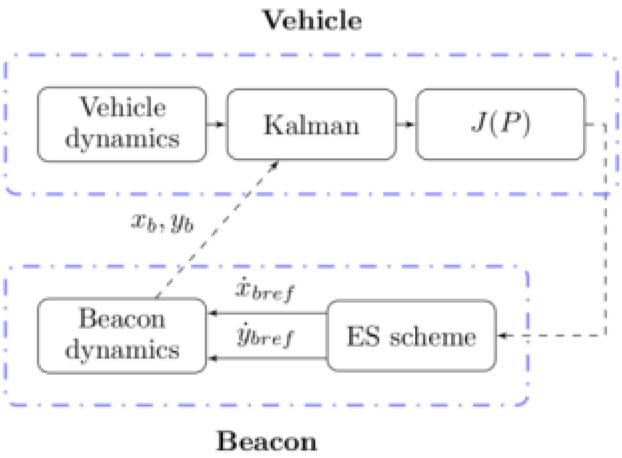

Figure 4.1 - Extremum seeking scheme

As it has been noted, in order to estimate its position using single range measurements, the vehicle has to travel sufficiently informative trajectories. This can disable the vehicle from doing other useful activities which require trajectories that are not informative enough. In order to avoid that, an approach with two vehicles, where one of them is a beacon, can be used. In that case, a mobile beacon, which knows its position accurately (from GPS), is responsible for travelling trajectories which will provide informative range measurements for the vehicle's navigation filter. Figure 4.1 depicts the main idea which enables better vehicle position estimation by using single beacon measurements. Mobile beacon sends its position (x_b, y_b) to the vehicle's Kalman filter used for navigation. Information generated in the navigation filter is then used to calculate cost function value J which gives a measure of observability. Current cost value is then sent to mobile beacon which tries to minimize it online by using extremum seeking scheme which steers the mobile beacon towards the minimum of cost function. The beacon again sends its position to the vehicle, thus closing the control loop. Range measurement used for determining vehicle's position is acquired during the communication cycle.

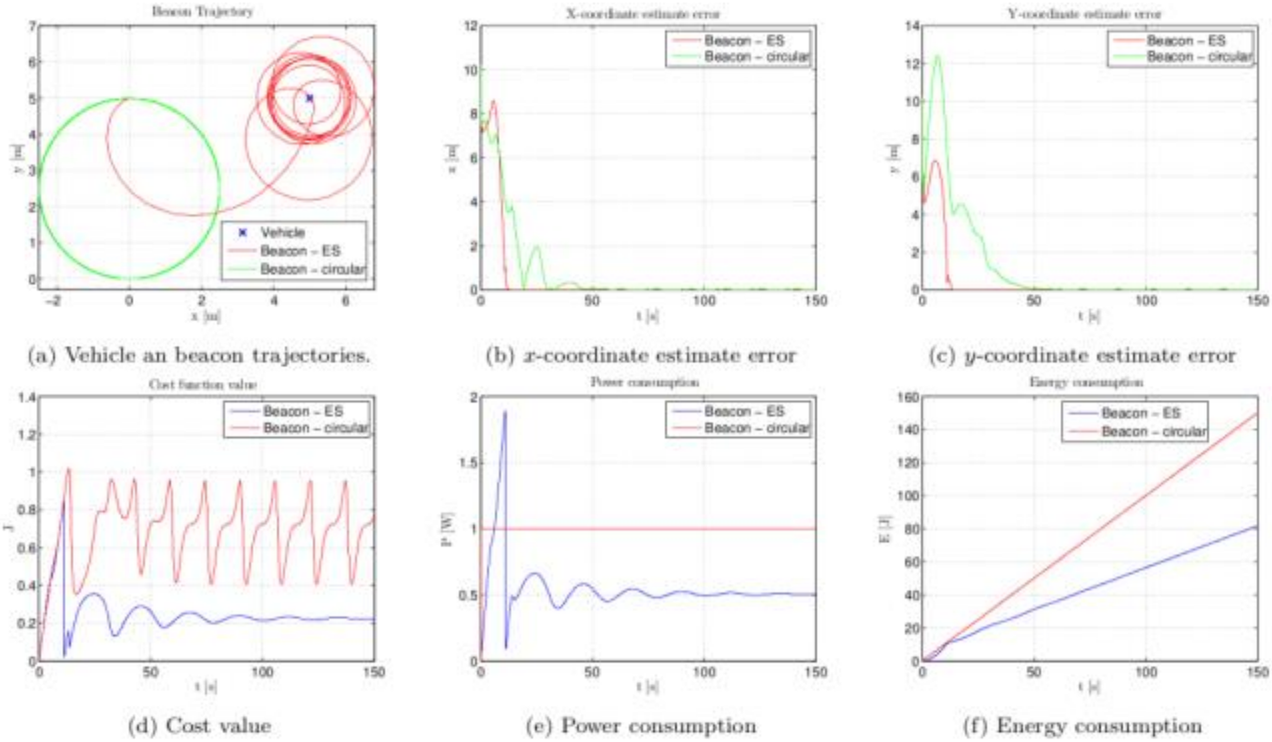

Figure 4.2 - Simulation results for the static vehicle scenario

The proposed algorithm was simulated for two different scenarios: stationary vehicle and mobile vehicle assuming curved trajectory. For both scenarios, we compared the basic case where mobile beacon executes constant speed circle trajectory which ensures system's observability, and the case where the mobile beacon is assuming the trajectory generated by the extremum seeking algorithm. Figure 4.2 and Figure 4.3 represent simulation results for a static vehicle and moving vehicle scenario, respectively.

Proposed mobile beacon trajectory generation method is particularly interesting for underwater application because of limited bandwidth of acoustic communication. In the extremum seeking scheme, the only data that needs to be transmitted over the acoustic link is the cost function value which is sent from the vehicle to the beacon, and the beacon position data needs to be sent to the vehicle. Extremum seeking is not a model based approach so it can be easily deployed on different types of vehicles. That can be particularly interesting in cases when model is difficult or impossible to obtain, i.e. in the case when the vehicle is replaced with a human diver. Another great advantage of extremum seeking is the fact that constant disturbances acting on vehicle, i.e. gravity, buoyancy or currents, are automatically compensated by the extremum seeking control loop. Furthermore, the proposed algorithm does not require knowledge of the vehicle's trajectory in advance. That can be particularly useful in real–life conditions when planned trajectories are known but currents that affect the vehicle and the mobile beacon change its desired trajectory and decrease optimality of solution.

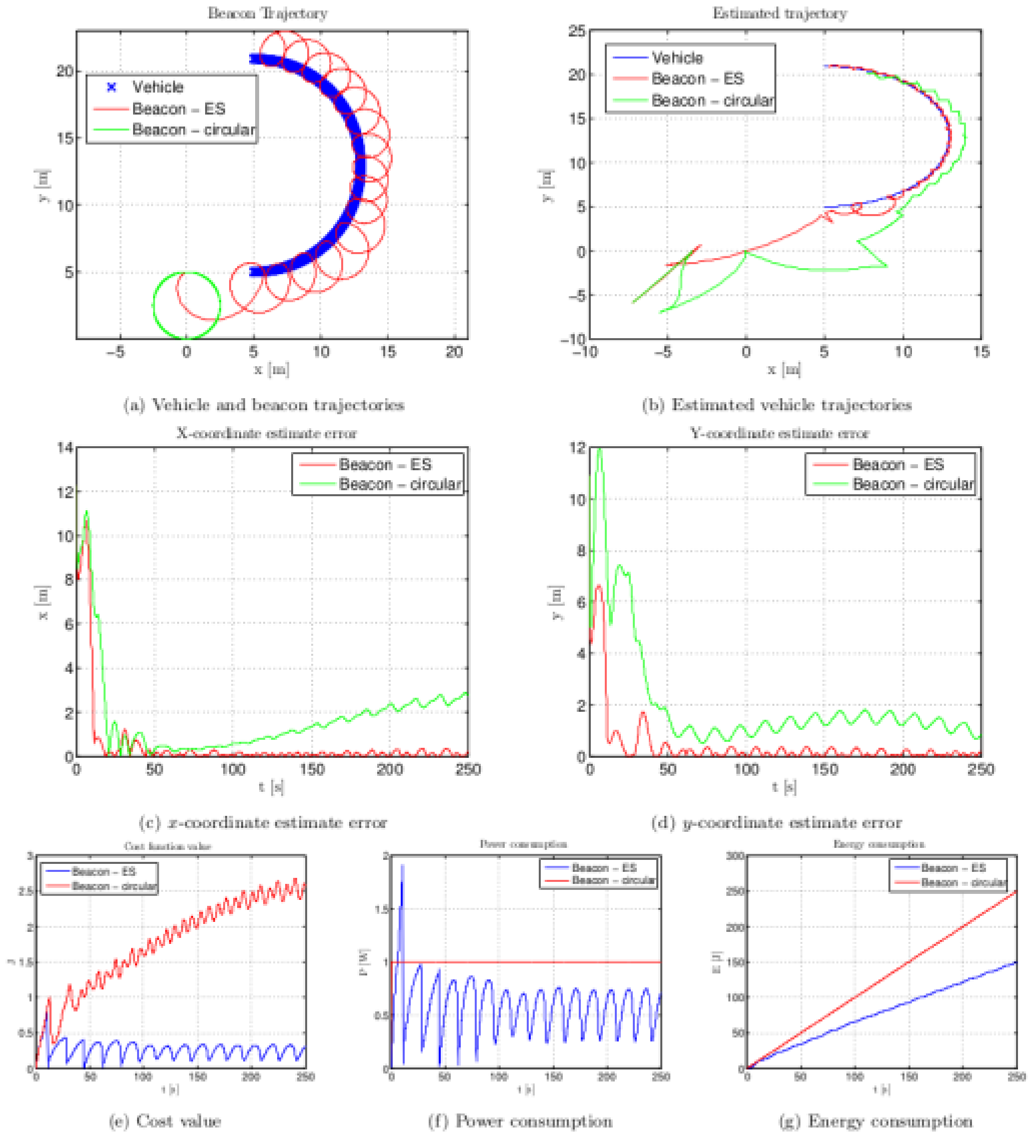

(a) Vehicle and beacon trajectories
(b) Estimated vehicle trajectories
(c) x-coordinate estimate error
(d) y-coordinate estimate error
(e) Cost value
(f) Power consumption
(g) Energy consumption

Figure 4.3 - Simulation results for the moving vehicle scenario.

5 Results

5.1 Single Beacon Navigation (IST)

In section 3, we considered the problem of finding optimal trajectories for vehicle positioning using range measurements to a known beacon. Now, we are interested in the problem of finding optimal trajectories of a vehicle, whose position is known, for an unknown target localization using range measurements to the unknown target. In the former problem, the vehicle position is unknown and the beacon is known, while in the latter problem the vehicle position is known and the target is unknown. However, in both of the cases the vehicle should optimize its trajectory either for self-localization or target localization.

In this section we discuss the implementation of the proposed method for the dual problem of cooperative target localization using range and depth information in 3D. We present a preliminary experimental result carried out with two autonomous marine vehicles of the Medusa class. Each vehicle has two side thrusters that can be independently controlled to impart forward and rotational motion. In addition, these are equipped with an attitude and heading reference system (AHRS) that provides measurement of body orientation and body-fixed angular velocity. Each vehicle is equipped with an acoustic Blueprint Seatrac data modem and ranging unit that is used for communications and also to measure the ranges among vehicles. Throughout the test, one of the Medusa vehicle was used as an underwater target, while the other Medusa was used as a surface vehicle interrogating the target.

In this mission the target vehicle was making a lawnmower trajectory starting from an unknown initial position without ocean currents. The target was operating at a constant depth of 1m and a constant body-speed of 0.2m/s and was navigated by combining the USBL and DVL information. All the computational algorithms such as optimal control and estimation were executed on board of the surface vehicle without the use of USBL angle measurements and the EKF was used as an estimator without USBL measurements. While estimating the target vehicle position, it had the access to both range and velocity vector of the target for every 1.5s. In this regards, this is not a truly range-only target localization. Figure 3.1 shows the overall block diagram of the algorithm.

At first, the planner solves the optimal control problem to find the optimal sequence of inputs for the next six samples, that is, it provides optimal values for the piecewise constant body-speed and the yaw-rate for the next six samples. In the next step, we apply the first optimal speed and yaw rate to the surface vehicle to drive to the next optimal location to acquire the new range measurement. The process is repeated at this new optimal location. Figure 5.1 shows the plot of the optimal trajectory of the surface vehicle and the estimated trajectory of the target. The target trajectory was estimated in two ways using the range-only information and the USBL information. Figure 5.2 shows the time-history of the optimal body-speed and the measured body speed. Note that at the beginning of the speed profile, the measured speed was saturated at the nominal speed 1m/s of the Medusa. This was due to the fact that the planner was carried with a nominal speed of 1.5m/s and a sampling time of 6s against the nominal speed of 1.0m/s and sampling time of 1.5s. This is also visible in the first leg of the surface vehicle trajectory in Figure 5.1. Figure 5.3 shows the time-history of the heading angle, while the Figure 5.4 represents the actual measurements, while Figure 5.5 shows the position variance.

Finally, the optimal FIM is given by $(m\sigma^{-2}/2)\, I_2$, where I_2 the identity matrix of size two, that is, the off diagonal elements of the FIM are zero, while the diagonal elements are equal and is given by $m\ \sigma^{-2}/2$. Consequently, the optimal determinant of FIM is $m\ 2\sigma^{-4}/4$. Figure 5.6 and Figure 5.7 show the plot of the evolution of the normalized FIM and normalized determinant versus number of samples, which is consistent with our theoretical findings.

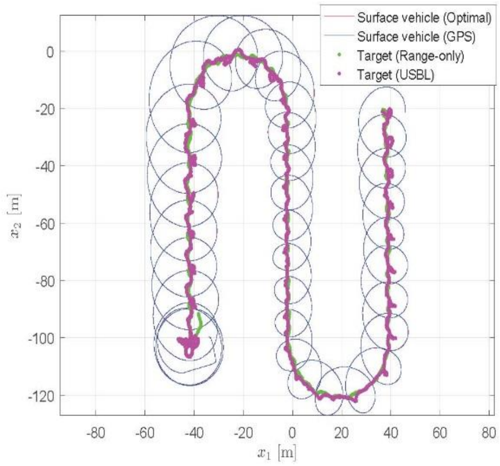

Figure 5.1 - The optimal ASV and estimated target trajectories

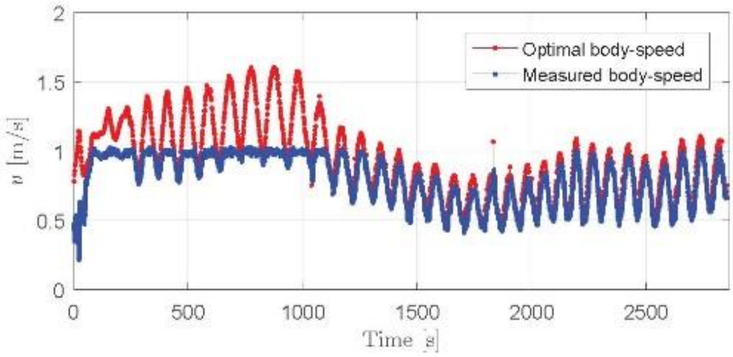

Figure 5.2 - Body-speed profile

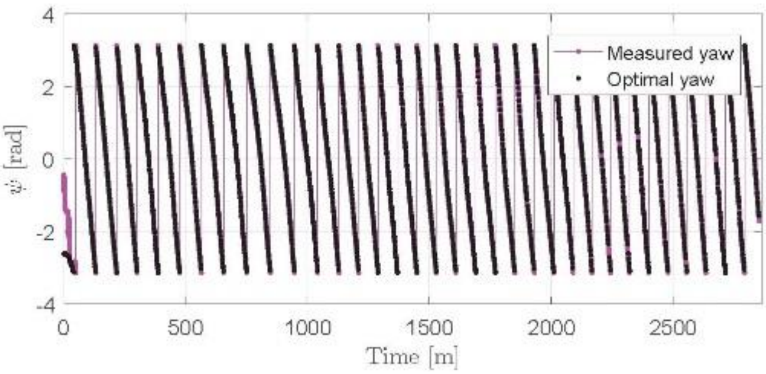

Figure 5.3 - Optimal heading angle time-history

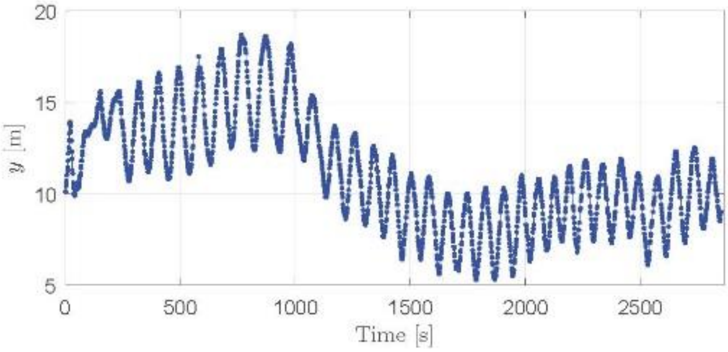

Figure 5.4 - The range measurements

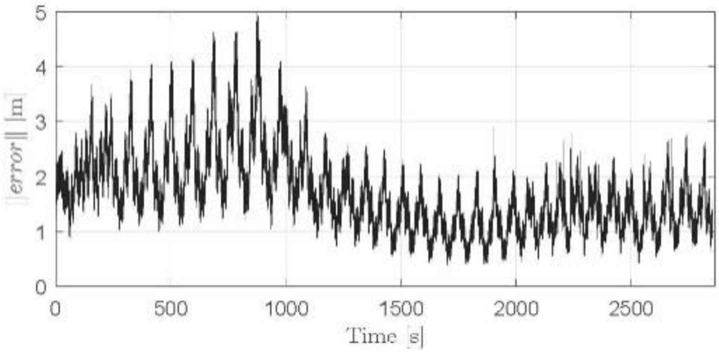

Figure 5.5 - The position variance

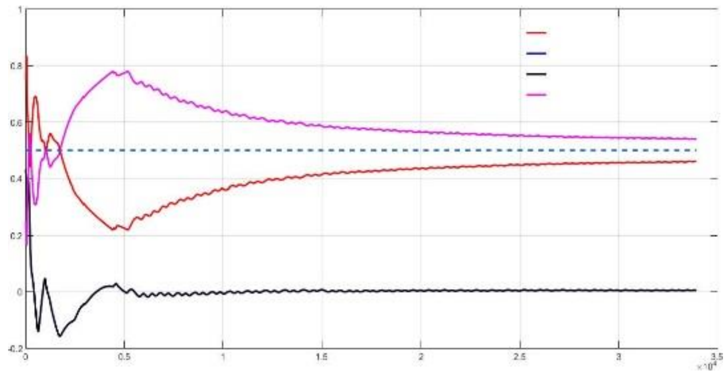

Figure 5.6 - Components of normalized FIM

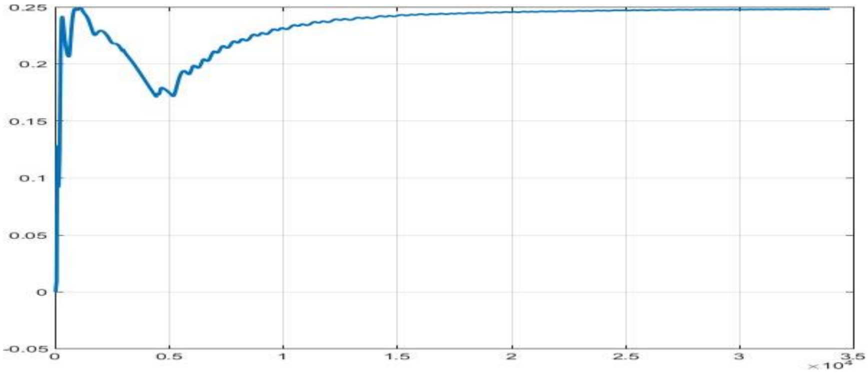

Figure 5.7 - Determinant of normalized FIM

5.2 Extremum Seeking (UNIZG-FER)

5.2.1 Tracking by using extremum seeking

In order to validate simulation results of extremum seeking tracking, during field trials, which took place in Biograd na Moru, Croatia in June 2015, algorithms for diver tracking using range-only measurements from an autonomous surface vehicle were tested. By using only range measurements surface vehicle was able to localize underwater target, i.e. diver, and stay on top of its position. That was achieved using three different extremum seeking algorithms. Test setup, shown in Figure 5.8, consisted of PlaDyPos platform with USBL modem which provided range measurements from VideoRay ROV that simulated the diver.

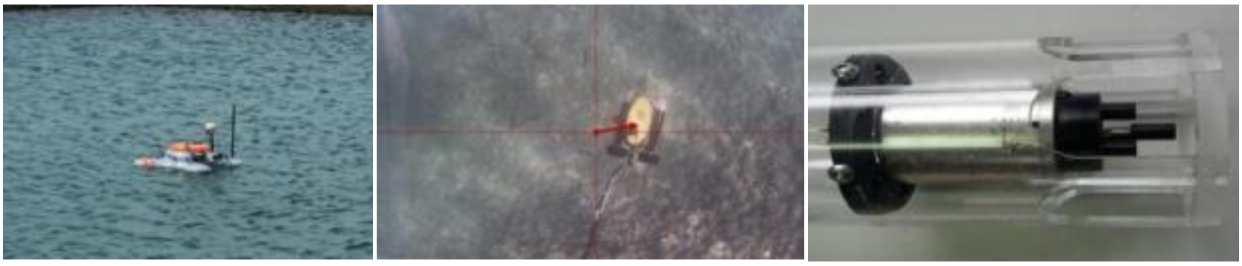

PlaDyPos *VideoRay ROV* *USBL with custom built cage*

Figure 5.8 - Systems used during extremum seeking experiments

The basic idea of extremum seeking control is to find control input u∗ which generates output y∗, where y∗ is minimum steady-state system output of unknown map y = F (u). Optimal control input u∗ is found by performing online gradient estimation. So in order to track the diver we want that the range between diver and surface vehicle is as low as possible.

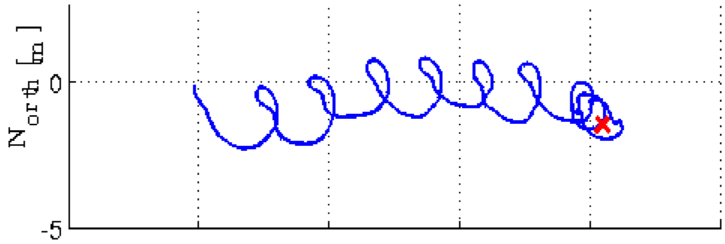

Trajectory

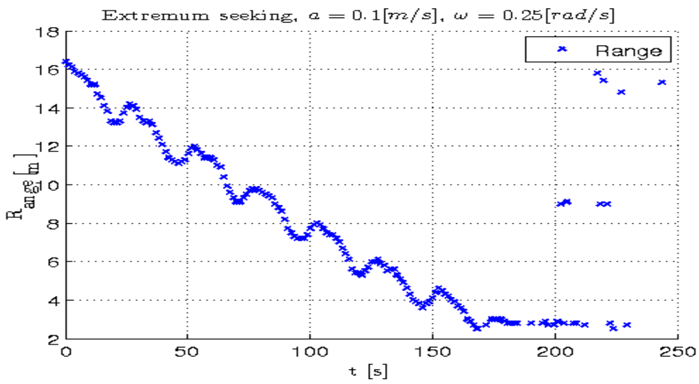

Range

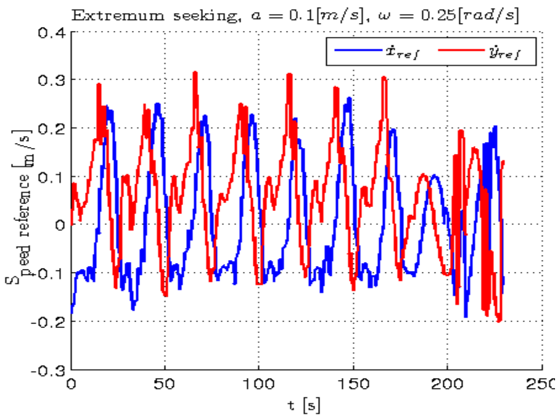

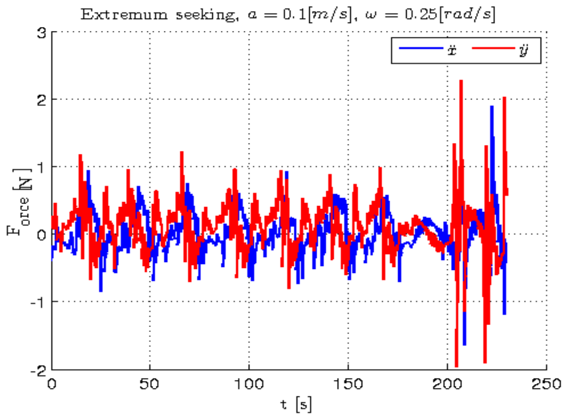

Speed *Force*

Figure 5.9 - Extremum seeking experimental results

Basic extremum seeking algorithm successfully localized underwater target, but alternative versions with EKF based gradient estimation showed better results due to the better speed of convergence. Some results are shown in Figure 5.9. As it can be seen from Figure 5.9, range measurements are sometimes affected by outliers caused by reflections from the underwater obstacles. Therefore, implementation of outlier rejection due to possible outliers is necessary.

Great advantage of extremum seeking is the fact that constant disturbances acting on vehicle, i.e. gravity, buoyancy, currents are automatically compensated by extremum seeking control loop which was supported by experimental data. Although range measurements are delayed, and there was very strong influence of wind, PlaDyPos successfully located underwater target position. Over 40 tests using extremum seeking algorithms were successfully conducted in changing conditions which shows robustness of approach.

5.2.2 Maximizing system observability by using extremum seeking

In order to validate simulation results, during validation trials, which took place in Biograd na Moru, Croatia in June 2015, algorithms for maximizing system observability by using extremum seeking described in were tested. Figure 5.10 depicts systems used during experiment: PlaDyPos surface vehicle, Buddy underwater vehicle both equipped with USBL modem.

PlaDyPos *Buddy* *USBL modem*

Figure 5.10 - Systems used during extremum seeking experiments

Figure 5.11 depicts first test scenario where underwater vehicle is virtual, and range measurements used to calculate cost function are simulated. It is clearly visible that we have a part where beacon vehicle approaches underwater vehicle while vehicle is static, and a second part of test where underwater vehicle is following straight line trajectory.

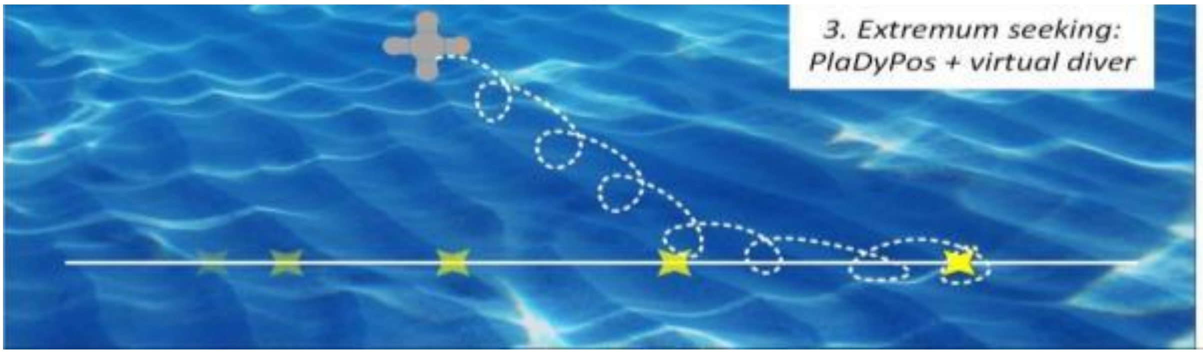

Figure 5.11 - Virtual target

Figure 5.12 depicts the same scenario with the difference that range measurements acquired through acoustic communication are used. It is important to note that such measurements are delayed. More detailed scenario descriptions are given in Tables 4.4.1 and 4.4.2.

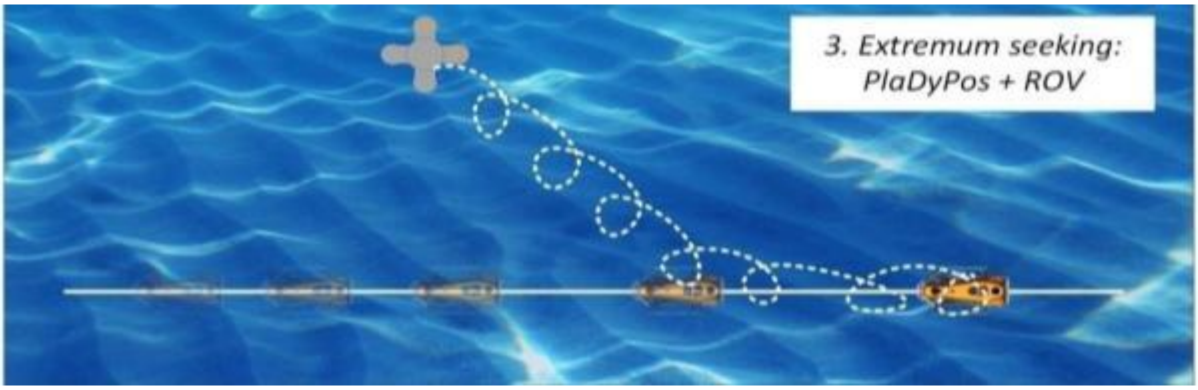

Figure 5.12 - Buddy as underwater target

Experiment:	Validation output:	Result:
1. Virtual target underwater is static, PlaDyPos tracks the target using the new ES method, range measurements simulated	PlaDyPos converges towards the virtual target	Pladypos successfully converges to virtual static target. Cost function is decreasing towards minimum
2. Virtual target underwater is moving along a straight line, PlaDyPos tracks the target using the new ES method, range measurements simulated	PlaDyPos converges towards the virtual target	Not tested due to time constraints imposed by bad weather

Table 4.4.1 Scenario 1: virtual underwater target, PlaDyPos as beacon vehicle

Experiment:	Validation output:	Result:
1. PlaDyPos converges towards static BUDDY (underwater) using the new ES method, range measurements obtained via acoustic link	PlaDyPos converges towards BUDDY	Pladypos successfully converges to position above Buddy vehicle. Cost function is decreasing towards minimum
2. PlaDyPos converges towards BUDDY (underwater) moving along a straight line, using the new ES method, range measurements obtained via acoustic link	PlaDyPos converges towards BUDDY	Pladypos successfully coto virtual static target. Cost function is decreasing towards minimum

Table 4.4.2. Scenario 2: BUDDY underwater, PlaDyPos as beacon vehicle

In this section results for scenario 1 where virtual underwater target was used and scenario 2 where Buddy vehicle was used as underwater vehicle are shown.

Figure 5.13-5.17 represent results of experiment 1 from scenario 1. Label “Beacon” denotes beacon vehicle trajectory, while label ”Single range” denotes underwater vehicle position estimate given by the extremely simple relative distance navigation filter whose covariance matrix P is also used for calculating observability cost shown in Figure 5.14. It is visible that proposed algorithm steers the cost towards its minimum and beacon vehicle towards circular trajectory around the vehicle. Such trajectory is known to have good observability properties when using single range measurements. In the end of the test, around 1100 seconds mark, algorithm was stopped in order to show how cost function grows unbounded when algorithm is not active.

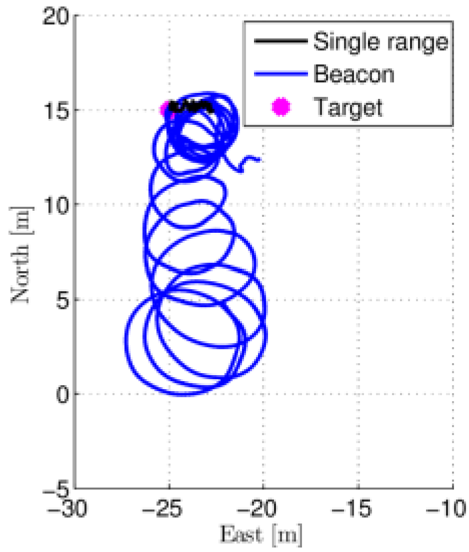

Figure 5.13 - Beacon and vehicle trajectories

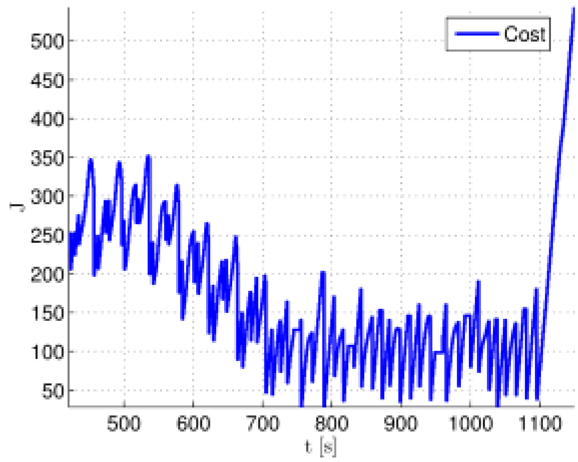

Figure 5.14 - Cost value

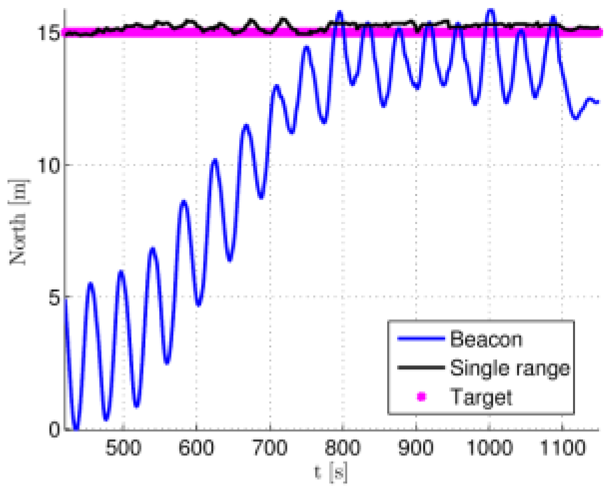

Figure 5.15 - North coordinate

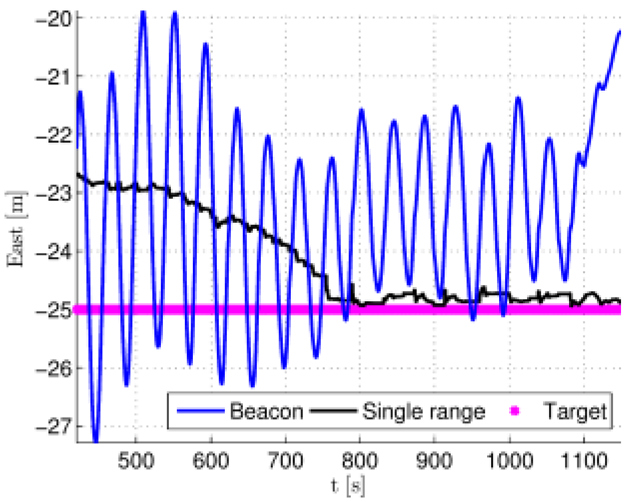

Figure 5.16 - East coordinate

Next, results for scenario 2 where Buddy vehicle was used as underwater vehicle are shown. Figure 5.17-20 show underwater vehicle and beacon trajectories for experiment 1 from scenario 2. In conducted experiments USBL measurements were used as ground truth, while ”Single range” label denotes underwater vehicle position estimate given by the simple relative distance navigation filter. Observability cost calculated from covariance matrix P is shown in Figure 5.18. It is visible that even in case of delayed acoustic measurements proposed algorithm steers the cost towards its minimum and beacon vehicle towards circular trajectory around the vehicle.

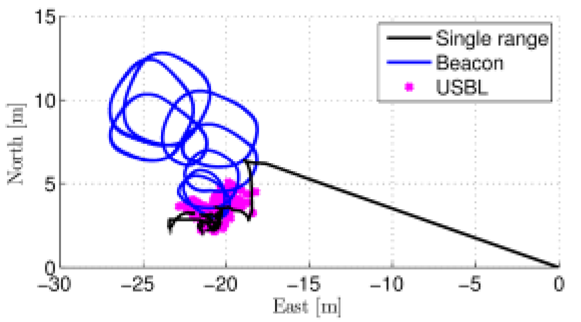

Figure 5.17 - Beacon and vehicle trajectories

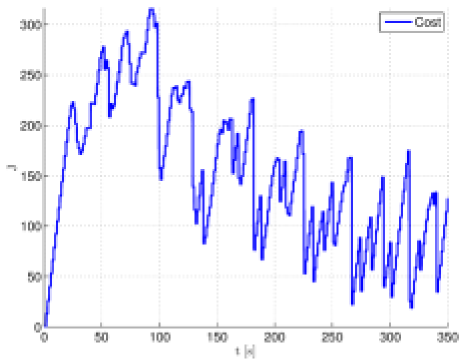

Figure 5.18 - Cost value

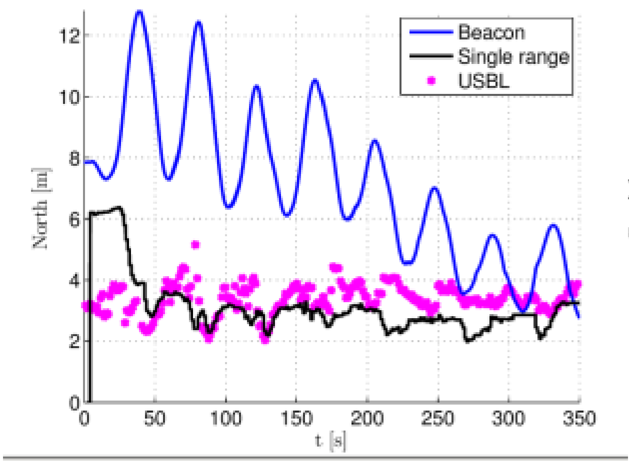

Figure 5.19 - North coordinate

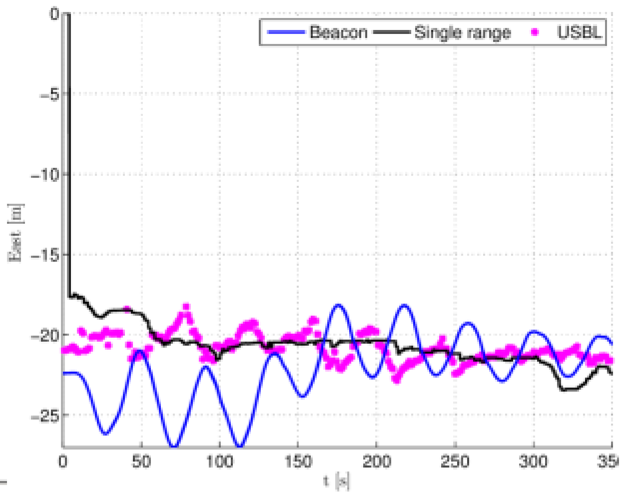

Figure 5.20 - East coordinate

Figure 5.21-24 show underwater vehicle and beacon trajectories for experiment 2 from scenario 2 where underwater vehicle executes straight line trajectory. Looking at observability cost shown in Figure 5.22. It is clear that cost value is bounded thanks to algorithm acting on beacon vehicle. As expected beacon vehicle moves along the underwater vehicle trajectory while simultaneously circulating in order to ensure good observability.

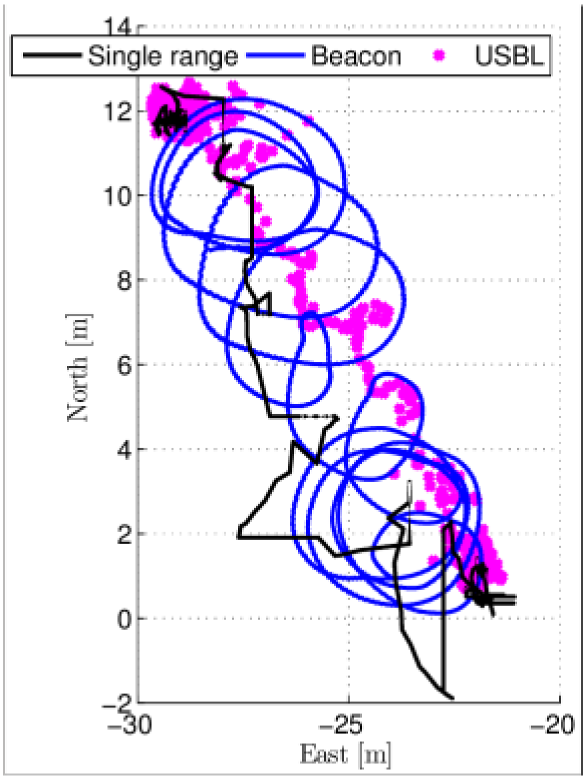

Figure 5.21 - Beacon and vehicle trajectories

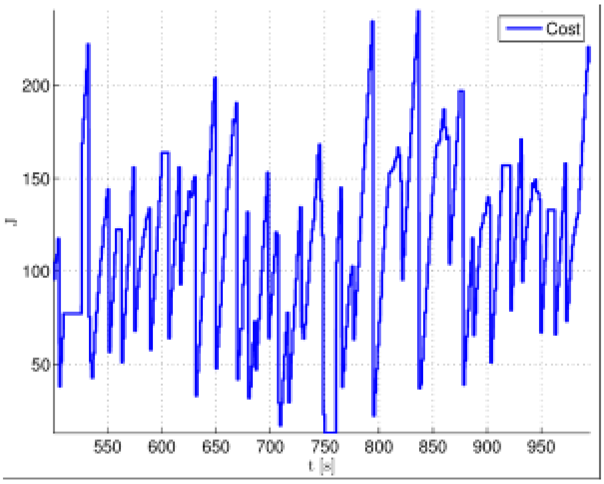

Figure 5.22 - Cost value

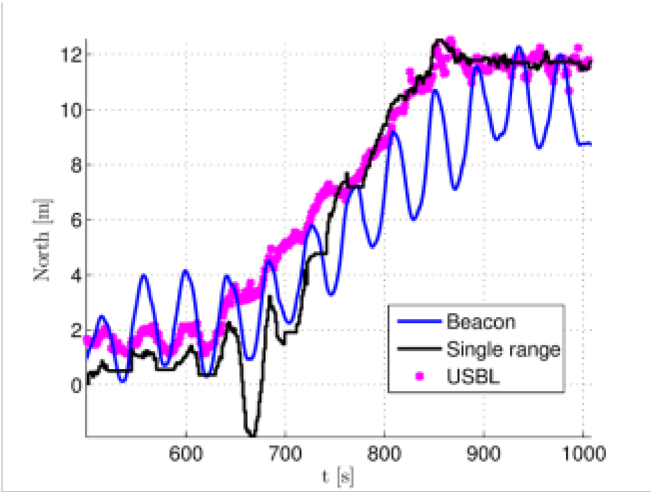

Figure 5.23 - North coordinate

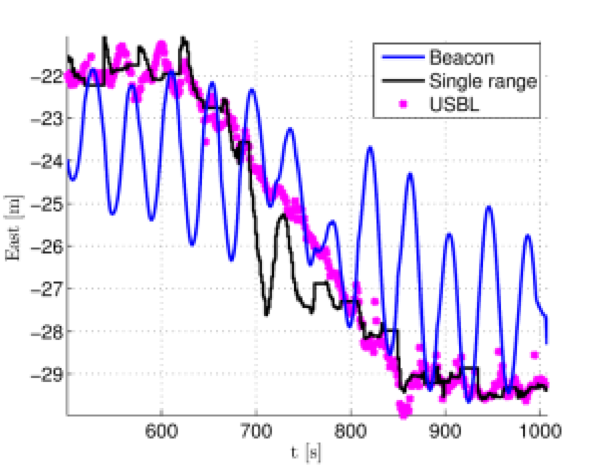

Figure 5.24 - East coordinate

6 Conclusions

This deliverable has described the design and implementation of several navigation algorithms in the scope of CADDY project, either resorting to USBL, DVL and exchanged data or to range and data only, providing the position of all the agents. Further testing will be done in October 2016, with the whole system working.

7 Literature

Crasta, N., D. Moreno-Salinas, M. Bayat, A. M. Pascoal, and J. A. Aranda. "Integrated motion planning, control and estimation for range-based marine vehicle positioning in the presence of unknown currents (under review)." *10th IFAC Conference on Control Applications in Marine Systems (CAMS).* Trondheim, Norway, 2016.

Moreno-Salinas, D., N. Crasta, M. Ribero, M. Bayat, A. M. Pascoal, and J. A. Aranda. "Integrated motion planning, control, and estimation for range-based marine vehicle positioning and target localization (under review)." *10th IFAC Conference on Control Applications in Marine Systems (CAMS).* Trondheim, Norway, 2016.